

Adaptive Frequency domain Affine Projection Equalizer of MIMO SC-FDMA System

Maha George Zia

(Electrical, College of Engineering/ Salahaddin University, Kurdistan Region, Iraq)

Abstract: Minimum mean-square error frequency domain equalizer (MMSE-FDE) is a promising technique that can handle the effect of a multi-path propagation channel and hence enhance the bit error rate (BER) performance in MIMO systems. MMSE-FDE is complex because its adapted weights require the calculation of channel state information (CSI) and signal-to interference plus noise power ratio (SINR). Both are considered as difficult tasks and important issues to obtain especially in long term evolution (LTE) and massive MIMO systems. To tackle these issues, adaptive affine projection frequency domain equalizer (AAPFDE) used within overlap-save method (OLSM) is proposed where its adapted weights do not depend on CSI or SINR. In this work, the proposed AAPFDE within OLSM is used in conjunction with a turbo decoder to enhance the BER performance in 8x8 and 16x16 MIMO SC-FDMA systems. Simulation results showed that MMSE-FDE outperforms the proposed AAPFDE in MIMO SC-FDMA system, but the proposed AAPFDE is simple and achieves good BER performance with less execution time.

Key Word: Frequency domain equalizer; MIMO; overlap-add, overlap-save; SC-FDMA.

Date of Submission: 09-10-2022

Date of Acceptance: 22-10-2022

I. Introduction

Frequency domain equalizer (FDE) [1-4] is preferable to the time domain equalizer [5-7] because it relies on Fast Fourier Transform (FFT) that requires less computations which results in less round-off error or noise. The received signals in MIMO SC-FDMA system are coupled both in time and space and they need efficient receiver to enhance the BER performance. This can be realized by frequency domain equalization schemes [7-10].

The literature [8] adopts two frequency domain equalization schemes, the joint complex regularized zero forcing scheme (JCZF) and MMSE scheme. Both schemes were used to analyze and investigate the performance improvement of MIMO SC-FDMA system under different carrier frequency offsets and channel models. Simulation results showed that JCZF scheme is highly competitive to MMSE scheme.

Different receiver algorithms and structures for MIMO SC-FDMA were proposed in [9]. One of those structures is a frequency domain MMSE equalization with spherical decoding. The main disadvantage of this designed receiver is its complexity. MMSE linear frequency domain equalization was also investigated for SC-FDMA transmission over MIMO THz channel [10]. Simulation results showed that MMSE linear frequency domain equalization is promising for practical THz systems.

As was mentioned earlier, most of researchers depend on minimum mean-square error frequency domain equalizer (MMSE-FDE) as a promising technique that can handle the effect of MIMO systems and have great BER performance improvement. The main disadvantage of MMSE-FDE is its complexity because its adapted weights require the calculation of channel state information (CSI) and signal-to interference plus noise power ratio (SINR). Both are considered as difficult tasks and important issues to obtain especially in long term evolution (LTE) and massive MIMO systems.

In this paper, these issues are tackled by designing adaptive affine projection frequency domain equalizer (AAPFDE) used within overlap-save method (OLSM) where its adapted weights do not depend on CSI or SINR values. The proposed AAPFDE within OLSM is used in conjunction with a turbo decoder to enhance the BER performance in 8x8 and 16x16 MIMO SC-FDMA systems in extended pedestrian A (EPA) channel. In summary, the motivation and contributions of this paper are:

1. Design a moderate receiver without requiring difficult parameters to estimate or depend on like CSI and SINR, where these parameters depend mainly on the channel type and its characteristics.
2. This moderate receiver depends on adaptive affine projection algorithm (APA) implemented in frequency domain equalizer within overlap-save method (OLSM). They are used in conjunction with a turbo decoder to enhance the BER performance of MIMO SC-FDMA system.
3. The AAPFDE weights are presented and compared with MMSE-FDE weights.
4. Demonstration of BER performances for 8x8 and 16x16 MIMO SC-FDMA systems in extended pedestrian

A (EPA) channel using both MMSE-FDE and AAPFDE.

- Simulation results are compared and showed that MSE-FDE outperforms the proposed AAPFDE in MIMO SC-FDMA system. but the proposed AAPFDE is simple and achieves good BER performance with less execution time.

II. MIMO SC-FDMA system structure

A proposed transceiver system model of MIMO SC-FDMA with $N_t \times N_r$ antennas is shown in Fig. 1. A frame of data bits of i -th transmit antenna ($i = 1, 2, \dots, N_t$) is encoded using a turbo encoder.

The coded bits are interleaved by using a random interleaver, and then they are QPSK modulated. A block of M data symbols is represented by \mathbf{x}_i , i.e., $\mathbf{x}_i = [x_{i,0}, x_{i,1}, \dots, x_{i,M}]$, serial-to-parallel converted and transformed to a frequency domain block $\mathbf{X}_i = [X_{i,0}, X_{i,1}, \dots, X_{i,M}]$ using M -point fast Fourier transform (FFT).

After using localized mapping, \mathbf{X}_i is mapped to $N > M$ subcarriers, i.e.

$$\mathbf{S}_i = \mathbf{A}\mathbf{X}_i. \tag{1}$$

where $\mathbf{A} = N \times M$ is the source allocation matrix of the localized mapping. The block \mathbf{S}_i is transformed to a time domain block \mathbf{s}_i via N -point inverse fast Fourier transform (IFFT) and returns the transmitted SC-FDMA signal vector as:

$$\mathbf{s}_i = \mathbf{F}_N^H \mathbf{A} \mathbf{F}_M \mathbf{x}_i = \mathbf{F}_N^H \mathbf{A} \mathbf{X}_i. \tag{2}$$

where $(\cdot)^H$ denotes the Hermitian operator. \mathbf{F}_N and \mathbf{F}_M are $N \times N$ and $M \times M$ FFT matrices, respectively.

Circular sub-channel matrices $\mathcal{H}_{i,j}$ are assumed to achieve circular property in the transmission. The received signal vector of j -th receiver antenna ($j = 1, 2, \dots, N_r$) is given by:

$$\begin{bmatrix} \mathbf{y}_1 \\ \vdots \\ \mathbf{y}_{N_r} \end{bmatrix} = \begin{bmatrix} \mathcal{H}_{1,1} & \dots & \mathcal{H}_{1,N_t} \\ \vdots & \ddots & \vdots \\ \mathcal{H}_{N_r,1} & \dots & \mathcal{H}_{N_r,N_t} \end{bmatrix} \begin{bmatrix} \mathbf{s}_1 \\ \vdots \\ \mathbf{s}_{N_t} \end{bmatrix} + \begin{bmatrix} \boldsymbol{\eta}_1 \\ \vdots \\ \boldsymbol{\eta}_{N_r} \end{bmatrix}. \tag{3}$$

where $\mathcal{H}_{i,j}$ is the frequency selective fading channel matrix between the i -th transmit antenna and j -th received antenna. The $\boldsymbol{\eta}_{N_r}$ is a complex valued additive white Gaussian noise with zero mean and unit variance.

At the receiver, after N -point FFT and demapping, the received signal vector in frequency domain is represents by:

$$\begin{bmatrix} \mathbf{Y}_1 \\ \vdots \\ \mathbf{Y}_{N_r} \end{bmatrix} = \begin{bmatrix} \mathbf{H}_{1,1} & \dots & \mathbf{H}_{1,N_t} \\ \vdots & \ddots & \vdots \\ \mathbf{H}_{N_r,1} & \dots & \mathbf{H}_{N_r,N_t} \end{bmatrix} \begin{bmatrix} \mathbf{S}_1 \\ \vdots \\ \mathbf{S}_{N_t} \end{bmatrix} + \begin{bmatrix} \boldsymbol{\Pi}_1 \\ \vdots \\ \boldsymbol{\Pi}_{N_r} \end{bmatrix}. \tag{4}$$

where $\mathbf{H}_{i,j}$ is $M \times M$ channel gain diagonal matrix, \mathbf{S}_i , and $\boldsymbol{\Pi}_j$ are the signal component, and noise component, respectively.

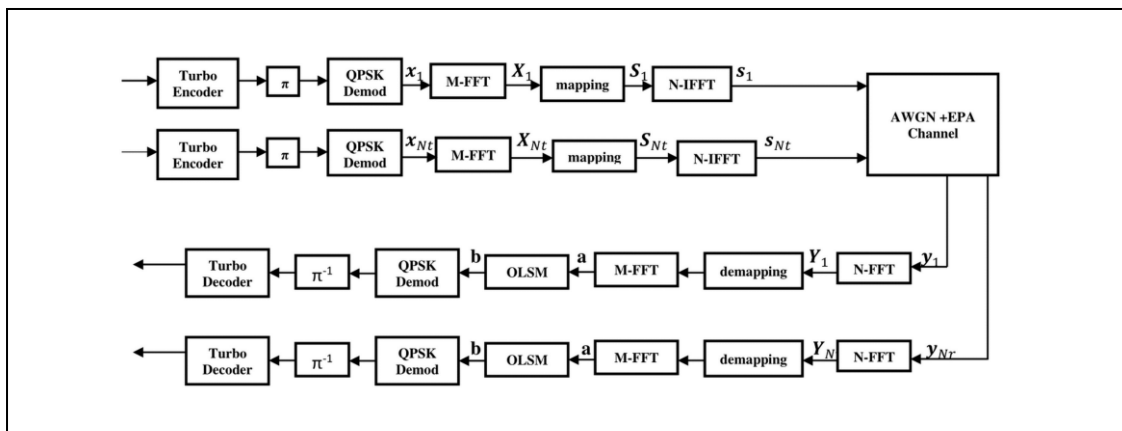


Fig.1 Proposed model of MIMO SC-FDMA

A. Turbo Decoding In Conjunction With Overlap-Save Method (OLSM) Block

The aim of his work is to design the overlap-save method (OLSM) block diagram in which the adaptive affine projection FDE is considered as the main part of it. The OLSM block diagram is shown in Fig. 2. The received SC-FDMA signal vector \mathbf{Y}_j is transformed again to time domain symbols using M -point IFFT and enters overlap-save method (OLSM) block [11-13]. The time domain vector at point (a) is divided into a

sequence of B -symbol blocks ($B \leq N_B$) with certain overlap of length N_B . N_B is the FFT size used to convert these blocks to a frequency domain. The frequency domain signal block is represented by:

$$\mathbf{R}_j(k) = \mathbf{H}_{i,j}(k)\mathbf{S}(k) + \mathbf{\Delta}_j(k), \quad k = 0, 1, \dots, N_B \quad (5)$$

where $\mathbf{H}_{i,j}(k)$, $\mathbf{S}(k)$, and $\mathbf{\Delta}_j(k)$ are respectively the channel gain, the signal component, and noise component due to AWGN. Now, each frequency component $\mathbf{R}_j(k)$ is multiplied by the adaptive affine projection frequency domain equalizer (AAPFDE) weight $\mathbf{w}_j(k)$:

$$\mathcal{R}_j(k) = \sum_j \mathbf{w}_j(k) \mathbf{R}_j(k). \quad (6)$$

Next, the equalized symbol blocks $\mathcal{R}_j(k)$ are transformed into time domain by using N_B -IFFT where the processed data blocks are combined to form \mathbf{D}_j vector at point (b). The vector \mathbf{D}_j is now entered to QPSK demodulator. The output of the demodulator is de-interleaved and is input to a turbo decoder [14-17].

I. PROPOSED METHOD

The proposed method is based on designing a receiver based on overlap-save method (OLSM) of MIMO SC-FDMA system as shown in Fig. 1 and Fig. 2. The main part of OLSM is the adaptive affine projection frequency domain equalizer (AAPFDE). The adaptive affine projection algorithm can be presented by:

Let the input vectors $\mathbf{X}(n)$ be $x(n), x(n-1), \dots, x(n-P_o+1)$ and the wanted output samples $\mathbf{d}(n)$ to be $d(n), d(n-1), \dots, d(n-P_o+1)$, where P_o is the projection order. The aim is to minimize the squared Euclidian norm of the difference between the updated weight vector $\mathbf{w}(n+1)$, and the previous weight vector $\mathbf{w}(n)$ which is given by equation [18-22]:

$$\boldsymbol{\zeta}(n) = \mathbf{w}(n+1) - \mathbf{w}(n). \quad (7)$$

The solution of (7) leads to the affine projection update equation [18-22]:

$$\mathbf{w}(n+1) = \mathbf{w}(n) + \mathbf{X}(n)(\mathbf{X}^T(n)\mathbf{X}(n))^{-1} \mathbf{e}(n). \quad (8)$$

where, the error estimation $\mathbf{e}(n)$ is the difference between the desired output and the output of the equalizer.

$$\mathbf{e}(n) = \mathbf{d}(n) - \mathbf{X}^T(n)\mathbf{w}(n). \quad (9)$$

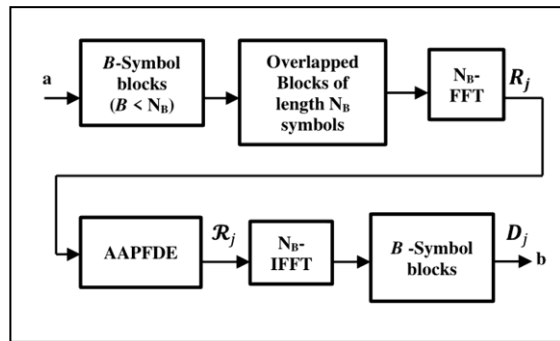


Fig.2 Overlap-save method block diagram

In practice, (9) can be written as:

$$\mathbf{w}(n+1) = \mathbf{w}(n) + \mu \mathbf{X}(n)(\mathbf{X}^T(n)\mathbf{X}(n) + \psi \mathbf{I})^{-1} \mathbf{e}(n). \quad (10)$$

Where, μ is the step size parameter, \mathbf{I} is $P_o \times P_o$ identity matrix, and ψ is a small positive constant to ensure the numerical stability of the algorithm when $\mathbf{X}^T(n)\mathbf{X}(n)$ is near singular matrix.

In this paper, the adaptive affine projection algorithm is applied in a frequency domain equalizer as AAPFDE. Therefore, both the input and the desired output of the equalizer are represented in frequency domain.

If $P_o = 1$, the APA is just normalized least mean square (NLMS) algorithm [18-22]. It is still less complex compared to MMSE algorithm where the tap weight vector adaptation $\mathbf{W}(K)$ in MMSE-FDE depends on channel state information and signal-to-interference plus noise power ratio (SINR) as described below [23]:

$$\mathbf{W}(K) = \frac{H^*(K)}{|H(K)|^2 + \kappa^{-1}}. \quad (11)$$

Where, $H(K)$ is channel state information (CSI), and κ^{-1} is signal-to-interference plus noise ratio (SINR)

III. Results and Discussion

The bit error rate (BER) performances of MIMO SC-FDMA system using the proposed AAPFDE and MMSE-FDE are evaluated by simulations. The turbo encoder is of rate 1/2 and its generator polynomial is represented as (5, [23 35], 23). QPSK data modulation is used. The extended pedestrian A (EPA) model is used

as a channel model [29]. It has seven Rayleigh fading taps at delays of 0, 30, 70, 90, 110, 190, and 410 ns, with relative power of 0, -1, -2, -3, -8, -17.2, and -20.8 dB, respectively. Five iterations are performed for both AAPFDE and turbo decoder. Table no 1 summarizes simulation parameters.

Block LU decomposition [24-28] was used to reduce the execution time of the matrix inversion of the adapted weights of both equalizers. The execution time of the proposed system using AAPFDE and MMSE-FDE was measured without and with block LU decomposition as listed in Table no2. By comparing (10) and (11), it can be noticed that the execution time without and with block LU decomposition for AAPFDE is less than MMSE-FDE because MMSE-FDE requires more time to find CSI as well as SINR.

Table no 1: Simulation parameters

Parameter	Value
System bandwidth	5 MHz
Interleaver type	random
SC-FDMA mapping	Localized
Channel coding	Turbo coding, rate 1/2
Channel model	EPA
MIMO Technique	Transmit diversity
Number of transmitter antennas	2, 4
Number of receiver antennas	2, 4
FFT size for overlap-save method N_B	32, 64
Adaptive FDE algorithm	Affine Projection, MMSE
Step size of AAPFDE	0.1, 0.01, 0.5
Projection order (M) of AAPFDE	1, 2, 3

Table no 2: Execution time without and with block LU decomposition

System Type with $N_B = 32$	without Block LU Decomposition (sec.)	with Block LU Decomposition (sec.)
8x8 MIMO SC-FDMA using AAPFD	301.84	161.49
16x16 MIMO SC-FDMA using AAPFDE	389.09	196.25
8x8 MIMO SC-FDMA using MMSE-FDE	408.34	218.06
16x16 MIMO SC-FDMA using MMSE-FDE	557.12	323.65

Fig. 3 shows the BER performances using three different step size values with projection order $Po = 2$ of AAPFDE. The FFT size in OLSM for both AAPFDE and MMSE-FDE is $N_B = 32$. Coding gain of 2 dB is observed at $BER=5 \times 10^{-2}$ between 8x8 and 16x16 MIMO SC-FDMA using MMSE-FDE. Also, at $BER=5 \times 10^{-2}$ for AAPFDE, coding gain values of 1.5 dB, 2 dB and 1.75 dB are observed for $\mu = 0.01, 0.1$ and 0.5 respectively between 8x8 and 16x16 MIMO SC-FDMA systems. It is seen that better performances can be obtained when using AAPFDE with small values of μ . Although good BER performances are obtained when $\mu = 0.01$ for AAPFDE, the BER performances of MMSE-FDE is much better than the BER performances of AAPFDE for 8x8 and 16x16 MIMO SC-FDMA systems.

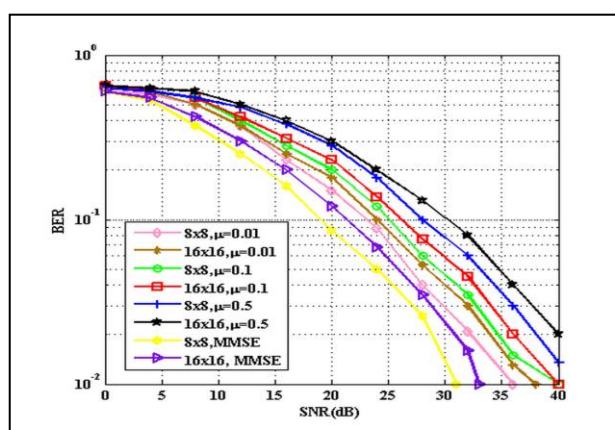


Fig.3 BER performances of 8x8 and 16x16 MIMO SC-FDMA systems using MMSE-FDE and AAPFDE (applied with different step size values, and $Po=2$). $N_B = 32$.

Three different projection order values with step size $\mu = 0.1$ of AAPFDE are illustrated in Fig.4. The FFT size in OLSM for both AAPFDE and MMSE-FDE is $N_B = 32$. Coding gain of 2 dB is observed at $BER=5 \times 10^{-2}$ using MMSE-FDE. The worse performance of AAPFDE is obtained at $BER = 5 \times 10^{-2}$ and $P_o = 1$, here the AAPFDE works as adaptive normalized least mean square (NLMS) equalizer with a performance gain of 1.25 dB obtained between 8x8 and 16x16 MIMO SC-FDMA systems. At the same $BER=5 \times 10^{-2}$, better Performances of AAPFDE can be obtained for higher order of P_o values where, coding gains of 1 dB and 2 dB are obtained at $P_o = 3$ and $P_o = 2$ respectively. By comparison of simulation results, MMSE-FDE still behaves better than AAPFDE (with $P_o = 3$) for 8x8 and 16x16 MIMO SC-FDMA systems.

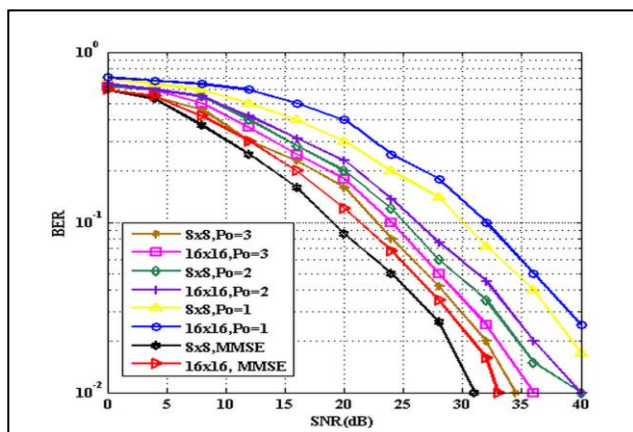


Fig.4 BER performances of 8x8 and 16x16 MIMO SC-FDMA systems using MMSE-FDE and AAPFDE (applied with different projection orders and $\mu = 0.1$). $N_B = 32$.

Two N_B values of 32 and 64 are chosen for both MMSE-FDE and AAPFDE as shown in Fig.5. These values are applied for 8x8 and 16x16 MIMO SC-FDMA systems. The AAPFDE is applied with step size value $\mu = 0.1$ and projection order $P_o = 2$. At $BER=5 \times 10^{-2}$, coding gains of values 2 dB, and 2 dB are obtained with $N_B = 32$ for MMSE-FDE and AAPFDE, respectively. The system performs worse at $N_B = 64$ with coding gains of values 1 dB, and 2 dB for MMSE-FDE and AAPFDE, respectively. It can be noticed that when N_B is small, better performances can be obtained. MMSE-FDE behaves much better than the proposed AAPFDE for both N_B values.

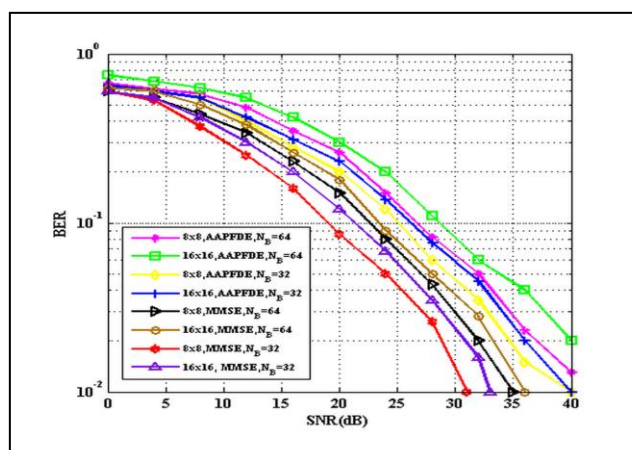


Fig.5 BER performances of 8x8 and 16x16 MIMO SC-FDMA system using different N_B values for MMSE-FDE and AAPFDE (with $\mu = 0.1$ and $P_o = 2$).

The equalized signal scatter plot using $N_B = 32$ for AAPFDE and MMSE-FDE are shown in Fig.6 and Fig.7 respectively. It can be noticed that MMSE-FDE has better scattering plot compared to the proposed AAPFDE.

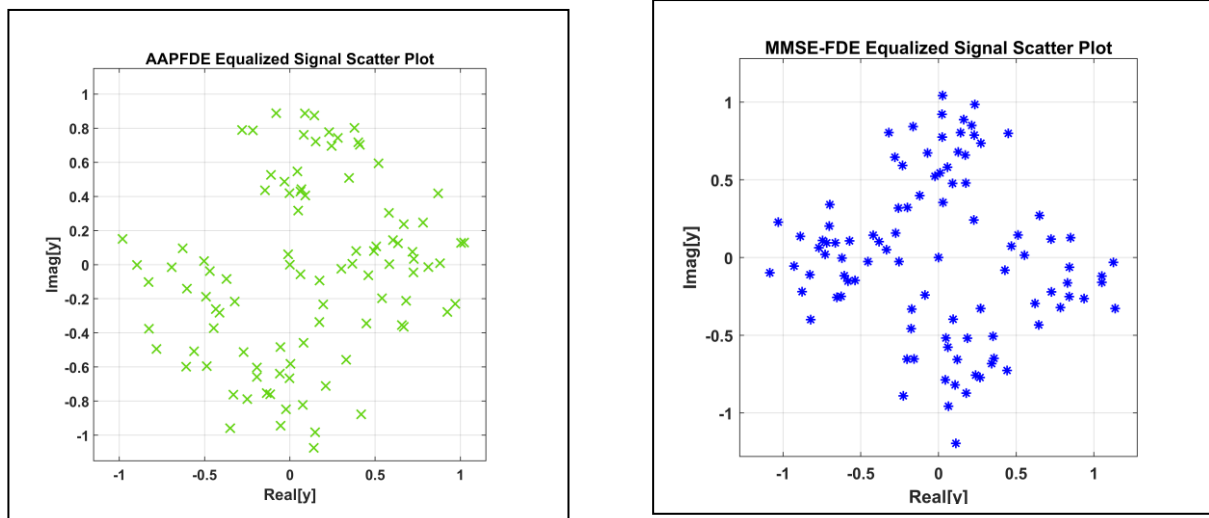


Fig. 6 AAPFDE equalized signal scatter plot Fig. 7MMSE-FDE equalized signal scatter plot

IV. Conclusion

Throughout this work, a moderate receiver was designed that depends on adaptive affine projection algorithm (APA) implemented a in frequency domain equalizer as AAPFDE within overlap-save method (OLSM). Demonstration of BER performances for both AAPFDE and MMSE-FDE in 8x8 and 16x16 MIMO SC-FDMA systems were evaluated by simulations. It was shown by simulation that 8x8 MIMO SC-FDMA has better performance than 16x16 MIMO SC-FDMA system using the proposed AAPFDE for small value of μ , moderate value of P_0 and small value of N_B . Also, MMSE-FDE performs much better and has better scatter plot than AAPFDE.

The objective of this work was to design a receiver with less complexity and execution time. MMSE-FDE outperforms the designed AAPFDE but at the expense of high complexity and hence high cost in the design. It was shown by simulation results that the complexity of MMSE-FDE comes from the calculation of CSI and SINR values to estimate its adapted weights while the designed AAPFDE does not require these values to estimate its adapted weights. Moreover, the execution time for the designed AAPFDE is less compared to MMSE-FDE without and with block LU decomposition. Therefore, the proposed AAPFDE is simple and achieves good BER performance in MIMO SC-FDMA systems.

References

- [1]. N. Iqbal, et al., "Adaptive Frequency-Domain RLS DFE for Uplink MIMO SC-FDMA," IEEE Transaction on Vehicular Technology, vol. 64, no. 7, pp. 2819–2833, July 2015.
- [2]. H-S. Wang, Fang-Biau Heng and Yu-Kuan Chang, "Novel Turbo Receiver for MU-MIMO SC-FDMA System," ETRI Journal, vol. 40, no. 3, pp.309–317, April 2018.
- [3]. M. Anbar, et al., "Iterative SC-FDMA Frequency Domain Equalization and phase Noise Mitigation," IEEE in Proceeding IEEE International Symposium on Intelligent Signal Processing and Communications Systems (ISPACS), Ishigaki, Japan, pp. 91–95, Nov. 2018.
- [4]. S. Sardar, et al., "A Framework for Iterative frequency Domain EP-Based Receiver Design," IEEE Transactions on Communications, vol. 66, no. 12, pp. 6478–6493, Dec. 2018.
- [5]. B. Dhivagar, K. Kuchi, and K. Giridhar, "An Iterative DFE Receiver for MIMO SC-FDMA Uplink," IEEE Communications Letters, vol.18, no. 12, pp. 2141–2144, Dec. 2014.
- [6]. K. Selvaraj, et al., "Low Complexity Linear Detection for Uplink Multiuser MIMO SC-FDMA Systems," Wireless Personal Communications, Springer, vol. 112, pp. 631–649, Jan. 2020.
- [7]. R. Zedka, T. Götthans, and R. Maršálek., "Spectral Efficient Time-Domain Equalization Single-Carrier System," in Proceeding IEEE 31st International Conference Radioelectronika, Brno, Czech Republic, pp.1-5, April 2021.
- [8]. M. Mustafa, et al., "MIMO SC-FDMA System Performance Investigation under Realistic channel Models," in Proceeding IEEE 36th National Radio Science Conference (NRSC), Port Said, Egypt, pp.145–152, April 2019.
- [9]. T. Hänninen, J. Ketonen and M. Juntti, "MIMO Detector for LTE/LTE-A Uplink Receiver," Springer, Journal of Signal Processing Systems, vol. 91, no. 5, pp.423–435, May 2019.
- [10]. V. Schram, et al., "Concepts for Indoor THz Communications Systems," in Proceeding IEEE 3rd International Workshop on Mobile Terahertz Systems (IWMTS), Essen, Germany, pp.1–5, July 2020.
- [11]. M. Najam, et al., "Hardware Implementation of Overlap-Save Based Fading Channel Emulator," IEEE Transactions on Circuits and Systems II, vol. 68, no. 3, pp.918–922, Sept. 2020.
- [12]. C. Li, H. K. Kwan, and X. Qin, "Revisiting Linear Convolution, Circular Convolution and Their Related Methods," in Proc. IEEE 13th International Congress on Image and Signal Processing, BioMedical Engineering and Informatics, Chengdu, China, pp.1124–1131, Oct. 2020.

- [13]. C. Bae and O. Gustafsson, "Overlap-Save Commutators for High-Speed Streaming Data Filtering," in Proceeding IEEE International Symposium on Circuits and Systems (ISCAS), Daegu, South Korea, pp.1-5, April 2021.
- [14]. M. Tomlinson, et al., "Error-Correction Coding and Decoding: Bounds, Codes, Decoders, Analysis and Application," Springer, 2017.
- [15]. F. Shahin, et al., "Performance Analysis of High Throughput MAP Decoder for Turbo Codes and Self Concatenated Convolutional Codes," *IEEE Access*, vol.7, pp. 138979-138093, Oct. 2019.
- [16]. N. Minallah, et al., "Analysis of Near-Capacity Iterative Decoding Schemes for Wireless Communications Using EXIT Charts," *IEEE Access*, vol.8, pp. 124424-124436, July 2020.
- [17]. M. Qiu, et al., "Analysis and Design of Partially- and Partially Parity-Coupled Turbo Codes," *IEEE Transactions on Communications*, vol. 69, no. 4, pp. 2107-2122, April 2021.
- [18]. K. Ozeki, "Theory of Affine Projection Algorithms for Adaptive Filtering," Springer, Japan, 2016.
- [19]. Z. Zheng, Z. Liu, and Y. Dong, "Steady-State and Tracking Analysis of the Improved Proportionate Affine Projection Algorithm," *IEEE Transactions on Circuits and Systems II*, vol. 65, no. 11, pp. 1793-1797, Nov. 2018.
- [20]. L. Shi, et al., "Variable Step-Size Widely Linear Complex-Valued Affine Projection Algorithm and Performance Analysis," *IEEE Transactions on Signal Processing*, vol. 68, no. pp. 5940-5953, Oct. 2020.
- [21]. S. Sitjongsataporn, S. Prongunch, and T. Wiangtong, "Diffusion Affine Projection Sign Algorithm based on QR-Decomposition," in Proceeding IEEE 9th International Electrical Engineering Congress (iEECON), Pattaya, Thailand, pp. 373-376, May 2021.
- [22]. M. Vilà; C. Alejandro López, and J. Riba, "Affine Projection Subspace Tracking," in Proceeding IEEE International Conference on Acoustics, Speech and Signal Processing, Toronto, Canada, pp. 3705-3709, June 2021.
- [23]. A Frequency Domain Joint MMSE-SIC Equalizer for MIMO SC-FDMA LTE-A Uplink," in Proceeding IEEE International Conference on Electronics and Communication Systems (ICECS), Coimbatore, India, pp.253-256, Feb. 2014.
- [24]. J. G. Gentle, "Matrix Algebra: Theory, Computations and Applications in Statistics," Springer, 2017.
- [25]. J. Liu, et al., "Spark-Based Large-Scale Matrix Inversion for Big Data Processing," *IEEE Access*, vol. 4, pp. 10042-10050, Jan. 2017.
- [26]. A. A. Muller, et al., "Computational Cost Reduction for N+2 Order Coupling Matrix Synthesis Based on Desnanot-Jacobi Identity," *IEEE Access*, vol. 4, pp.2166-2176, May 2016.
- [27]. L. Ma, et al., "QR Decomposition-Based Matrix Inversion for High Performance Embedded MIMO Receivers," *IEEE Transaction on Signal Processing*, vol. 59, no. 4, pp. 1858-1867, April 2011.
- [28]. M. A. M. Albreem, et al., "On Approximate Matrix Inversion Methods for Massive MIMO Detectors," *IEEE Wireless Communications and Networking Conference (WCNC)*, Marrakesh, Morocco, pp.1-6, 2019
- [29]. ETSI TS 136 116 V14.3.0 (2017), "LTE; Evolved Universal Terrestrial Radio Access (E-UTRA), Relay Radio Transmission and Reception".

Maha George Zia. "Adaptive Frequency domain Affine Projection Equalizer of MIMO SC-FDMA System." *IOSR Journal of Electronics and Communication Engineering (IOSR-JECE)* 17(5), (2022): pp 33-39.